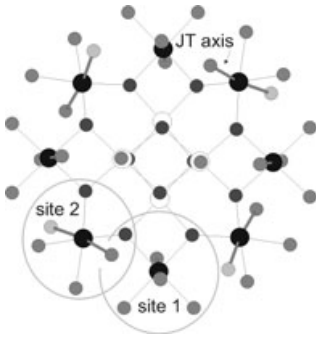

Figure 1. Structure of the core of Mn_{12}-acetate (view along the S_4 axis). For clarity only the first coordination sphere of the Mn ions is drawn. The single-ion Jahn–Teller (JT) axes are represented by thick bonds. Mn^{4+}: white, Mn^{3+}: black, μ_3-O^{2-}: dark gray, OAc: medium gray, H_2O: light gray. The two specific sites 1 and 2 are used in the data analysis and discussion.

Single-Molecule Magnets

Effect of Pressure on the Magnetic Anisotropy in the Single-Molecule Magnet Mn_{12}-Acetate: An Inelastic Neutron Scattering Study**

*Andreas Sieber, Roland Bircher, Oliver Waldmann, Graham Carver, Grégory Chaboussant, Hannu Mutka, and Hans-Ulrich Güdel**

Mn_{12}-acetate is the prototype of a class of polynuclear transition metal complexes known as single-molecule magnets (SMMs). These spin clusters exhibit new phenomena such as slow relaxation and quantum tunneling of magnetization (QTM) at low temperature,[1,2] and this discovery, about a decade ago, triggered a flurry of interdisciplinary research in physics and chemistry. Mn_{12}-acetate was the first SMM discovered, and its properties have been thoroughly studied by many different techniques. As shown in Figure 1, it is composed of a tetrahedral core of oxygen-coordinated Mn^{4+} ions, which are surrounded by a ring of eight Mn^{3+} ions with oxo and acetate coordination.[3] Dominant antiferromagnetic interactions between the Mn^{4+} and Mn^{3+} ions lead to an $S = 10$ ground state.[4] The Mn^{3+} coordination environment is Jahn–Teller-distorted; the elongated Mn–O bonds are emphasized in Figure 1. The concerted action of the resulting Mn^{3+} single-ion anisotropies leads to an overall easy-axis-type anisotropy of the $S = 10$ cluster ground state, which can be expressed by Equation (1).

$$\hat{H}_{ZFS} = D[\hat{S}_z^2 - {}^1/_3 S(S+1)] + B_4^0 \hat{O}_4^0$$
where
$$\hat{O}_4^0 = 35\hat{S}_z^4 - 30S(S+1)\hat{S}_z^2 + 25\hat{S}_z^2 - 6S(S+1) + 3S^2(S+1)^2 \quad (1)$$

As a result the $S = 10$ ground state splits in zero field into eleven $\pm M_S$ sublevels, of which $M_S = \pm 10$ are lowest in energy. An energy barrier between the plus and minus M_S sublevels is thus built up (Figure 2). Inelastic neutron scattering (INS), for which $\Delta M_S = \pm 1$ transitions are allowed, is eminently suited for the direct measurement of this splitting pattern in zero field.[5] The physical properties of Mn_{12}-acetate can be tuned by chemical variation[6,7] or by physical perturbations such as an external magnetic field or pressure.[8,9] Here we report the first spectroscopic study of the anisotropy splitting of Mn_{12}-acetate under hydrostatic pressure up to 12 kbar. From magnetization experiments it was earlier concluded that the anisotropy barrier increases with increasing pressure.[8] From the observed acceleration of the

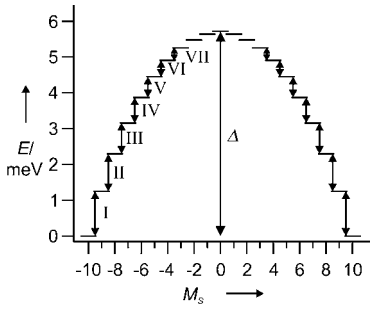

Figure 2. Axial anisotropy splitting and energy barrier Δ of the $S = 10$ ground state. The double arrows correspond to the observed $\Delta M_S = \pm 1$ INS transitions.

[*] A. Sieber, R. Bircher, O. Waldmann, G. Carver, Prof. H.-U. Güdel
Department of Chemistry and Biochemistry
University of Bern
3000 Bern 9 (Switzerland)
Fax: (+41) 31-631-4399
E-mail: hans-ulrich.guedel@iac.unibe.ch
G. Chaboussant
Laboratoire Léon Brillouin (LLB-CNRS-CEA)
CEA Saclay
91191 Gif-sur-Yvette Cedex (France)
H. Mutka
Institut Laue-Langevin
6 rue Jules Horowitz, BP 156, 38042 Grenoble Cedex 9 (France)

[**] This work was financially supported by the Swiss National Science Foundation (NFP 47) and the European Union (TMR Quemolna MRTN-CT-2003-504880).

Supporting information for this article is available on the WWW under http://www.angewandte.org or from the author.

 DOI: 10.1002/ange.200500171

magnetization relaxation it was further postulated that pressure induces partial conversion of the normal, slow-relaxing (SR) Mn_{12}-acetate molecules into a faster relaxing (FR) species.[9] Since INS allows the identification and quantitative characterization of individual species, we expect to clarify and quantify these points, which are important for understanding the mechanism and structural origin of slow magnetic relaxation in Mn_{12}-acetate.

Figure 3 shows the relevant section of the 2.5 K INS spectrum of a fully deuterated sample of Mn_{12}-acetate for the full accessible pressure range, measured on IN5 at the ILL in

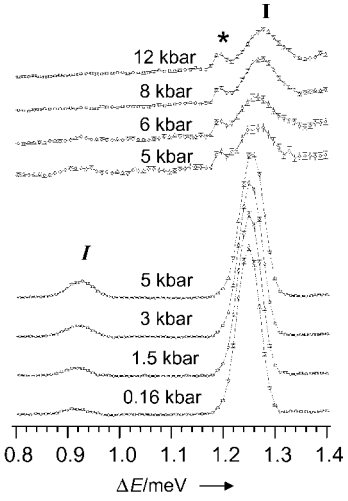

Figure 3. INS spectra at 2.5 K of Mn_{12}-acetate for the indicated pressures. The spectra correspond to the sum of all the scattering angles and are normalized to the elastic intensity. The upper four spectra were obtained with the clamp cells. The lower signal-to-noise ratios in the clamp-cell data originate from the higher background. The labels I and *I* refer to the $\pm 10 \rightarrow \pm 9$ transition (Figure 2) of the majority and minority species, respectively. The asterisk marks a spurion.

Grenoble. At 2.5 K the only allowed INS transition is $M_S = \pm 10$ to ± 9. Besides the major peak I around 1.25 meV, we observe a weaker peak *I* around 0.92 meV. The intensity ratio of the two peaks is clearly pressure dependent, and we assign the weak peak to a minority species. Its fraction increases from 3.8 % at ambient pressure to 11.1 % at 5 kbar, and this conversion is reversible. Above 6 kbar the minority peak is no longer observable in our spectra, most likely due to inhomogeneous broadening and the lower signal-to-noise ratio in the high-pressure clamp cells. Furthermore, a shift of the INS peak positions to higher energies with increasing pressure is evident for both species. Figure 4 shows the pressure dependence of the INS spectrum at 23 K. At this temperature all levels are thermally populated and seven transitions (labeled I to VII in Figure 4) within the zero-field split (ZFS) $S = 10$ ground state are observed. The 5 kbar pattern was measured at four temperatures from 2.5 K to 23 K, and this allowed the peaks originating from the two different species to be identified (cf. Supporting Information). The pressure dependent peak positions of the majority and minority species are listed in Tables S1 and S2, respectively, in the Supporting Information.

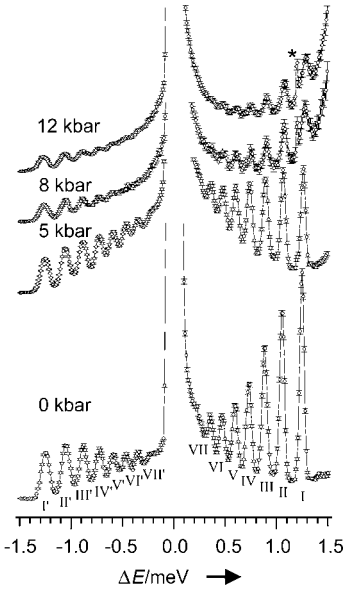

Figure 4. INS spectra at 23 K of Mn_{12}-acetate for the indicated pressures. The spectra correspond to the sum of all the scattering angles and are normalized to the elastic intensity. The lower signal-to-noise ratios at 8 and 12 kbar originate from the higher background of the clamp cells. The labeling of the peaks corresponds to the scheme adopted in Figure 2. The data at ambient pressure are taken from ref. [5]. The asterisk marks a spurion.

It is straightforward to assign the majority species in our INS spectra to the normal, SR Mn_{12}-acetate molecules with the structure shown in Figure 1. The minority species with a significantly smaller anisotropy is assigned to a FR isomer with a different structure. The observed fraction of 3.8 % at ambient pressure is in good agreement with the value of 5 % derived from ac susceptibility measurements.[10]

For ambient pressure the ZFS of the majority species has been studied previously in great detail by INS with higher instrumental resolution.[5] In addition to the D and B_4^0 parameters in Equation (1), it was possible to quantify two higher order terms which lead to deviations from the pattern in Figure 2. In the present study we concentrate on transitions I–IV, and these are essentially unaffected by the higher order terms and are sufficient to determine both D and B_4^0 accurately. The results of least-squares fits of the eigenvalues of Equation (1) to the experimental energies are given in Tables S1 and S2 in the Supporting Information. The variation of D as a function of pressure for both species is shown in Figure 5. In analogy to other Mn_{12} systems,[6,7] we assume an $S = 10$ ground state for the minority species, which is in good agreement with our INS data. The pressure dependence of D of the SR species is in good agreement with the values given in ref. [8]. The 2.1 % increase in $|D|$ between ambient pressure and 12 kbar is significant. B_4^0 is pressure-independent within experimental accuracy, and thus this parameter was kept constant in the analysis.

D in Equation (1) can be related to the anisotropy of the individual Mn^{3+} ions by Equation (2) where the projection

$$D = 2 \sum_{i=1}^{2} a_i D_{Mn^{3+},i} (3 \cos^2 \alpha_i - 1) \qquad (2)$$

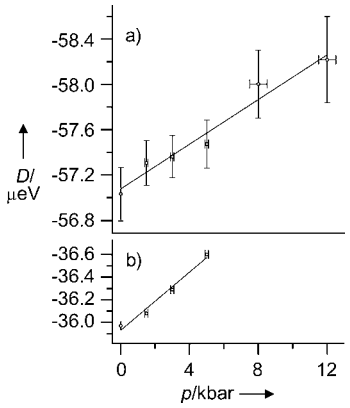

Figure 5. Variation of D as a function of hydrostatic pressure for a) the majority species and b) the minority species.

coefficient $a_i = 0.02845$[3] and α_i is the projection angle of the respective single-ion anisotropy axis (Jahn–Teller axis) on the cluster-anisotropy axis (S_4 axis). The two distinct Mn^{3+} sites with $i = 1$ and 2 (Figure 1) have values of $\alpha_1 = 11°$ and $\alpha_2 = 37°$, respectively, and thus contribute differently to D. In a recent pressure study of another SMM containing Mn^{3+}, $[Mn_4O_3Br(OAc)_3(dbm)_3]$ (dbm = dibenzoylmethane) or Mn_4 in short, $|D|$ was found to decrease by 3.8% between ambient pressure and 12 kbar.[11] This was ascribed to a tilting of the Jahn–Teller axes under pressure, which leads to a decrease in the $(3\cos^2\alpha_i - 1)$ factor in Equation (2). The situation is different in Mn_{12}-acetate, where the observed increase in $|D|$ can be explained by an increase in $|D_{Mn^{3+},i}|$. Using the angular overlap model (AOM) as in ref. [12] and assuming the same compressibility for all Mn^{3+}–O bonds ($d_{12\,kbar}/d_{0\,kbar} = 0.9975$),[11] we can calculate the pressure dependence of $D_{Mn^{3+},i}$ by scaling the AOM parameters with the Mn–O distances. Assuming constant α_i in Equation (2) (isotropic compression), we calculate an increase in $|D|$ of 2.2% between ambient pressure and 12 kbar. The excellent agreement with the experimental value of 2.1% is fortuitous, but the calculation clearly reveals that an increase in the single-ion anisotropy under pressure can explain the observed pressure dependence. As seen in Figure 5b, $|D|$ increases about twice as strongly with pressure in the minority species, but here, too, the main effect is an increase in single-ion anisotropies with increasing pressure.

For a number of Mn_{12}-acetate derivatives FR minority species have been identified and studied in detail. In all cases the activation energy for the magnetization relaxation Δ_{rel} is reduced by about 40% compared to the SR species, but with regard to the anisotropy barrier Δ (Figure 2), two different groups can be distinguished. In the first group the reduction of Δ is about an order of magnitude smaller than the reduction of Δ_{rel}.[6] This is ascribed to a switching of the Jahn–Teller axis of one of the Mn^{3+} ions on site 2 towards the μ_3-oxo bridge (Figure 1). In the second group the reduction of Δ is similar to that of Δ_{rel},[7] and a rather unusual coordination geometry (compressed octahedron) at one Mn^{3+} ion on site 2 was proposed. From our INS data we derive $\Delta = 5.75$ and 3.7 meV at ambient pressure for the SR and FR species, respectively. The reduction of Δ is thus similar to the reduction of the relaxation barrier from $\Delta_{rel} = 5.6$ meV for the SR to $\Delta_{rel} = 3.5$ meV for the FR species.[13] This would place Mn_{12}-acetate in the second group, but additional structural information on the FR species in Mn_{12}-acetate would be desirable.

High-resolution INS allows the simultaneous direct measurement of the anisotropy splitting and its pressure dependence in the $S = 10$ ground state of the two molecular species in Mn_{12}-acetate. From the INS data we clearly see a transformation of the SR into the FR species under pressure. The axial anisotropy of both species increases with increasing pressure, in striking contrast to the situation found in Mn_4, for which a decrease is observed. Apparently, there are no general rules for the pressure dependence of the axial anisotropy in SMMs, though we could provide a consistent explanation for both Mn_{12}-acetate and Mn_4.

Experimental Section

A fully deuterated, polycrystalline sample of Mn_{12}-acetate was synthesized according to ref. [14].

INS measurements were performed on the high-resolution time-of-flight spectrometer IN5 at the Institut Laue-Langevin in Grenoble, France. A neutron wavelength of $\lambda_i = 5.9$ Å (FWHM = 57 μeV) was used. Data treatment involved the calibration of the detectors with a vanadium spectrum. The time-of-flight to energy conversion and data reduction were performed with the standard program INX at the ILL.

A standard ILL continuously loaded high-pressure He gas cell, loaded with 4.3 g of Mn_{12}-acetate, was used for pressures $p = 0.16(1)$, 1.5(1), 3.0(1), and 5.0(1) kbar. For $p = 5.0(5)$, 6.0(5), and 8.0(5) kbar the standard ILL 10 kbar high-pressure clamp cell (0.6 g sample) and for $p = 12.0(5)$ kbar the standard ILL 15 kbar high-pressure clamp cell (0.4 g sample) were used with FC-75 (fluorinated hydrocarbon, 3M) as pressure-transmitting medium. An ILL orange cryostat was used for cooling.

Received: January 17, 2005
Revised: March 30, 2005
Published online: June 7, 2006

Keywords: high-pressure chemistry · inelastic neutron scattering · Jahn–Teller distortion · magnetic properties · manganese

[1] R. Sessoli, D. Gatteschi, A. Caneschi, M. A. Novak, *Nature* **1993**, *365*, 141 – 143.
[2] D. Gatteschi, R. Sessoli, *Angew. Chem.* **2003**, *115*, 278 – 309; *Angew. Chem. Int. Ed.* **2003**, *42*, 268 – 297.
[3] A. Cornia, R. Sessoli, L. Sorace, D. Gatteschi, A. L. Barra, C. Daiguebonne, *Phys. Rev. Lett.* **2002**, *89*, 257201.
[4] G. Chaboussant, A. Sieber, S. Ochsenbein, H.-U. Güdel, M. Murrie, A. Honecker, N. Fukushima, B. Normand, *Phys. Rev. B* **2004**, *70*, 104422.
[5] R. Bircher, G. Chaboussant, A. Sieber, H.-U. Güdel, H. Mutka, *Phys. Rev. B* **2004**, 70, 212413.
[6] S. M. J. Aubin, Z. Sun, E. M. Rumberger, D. N. Hendrickson, G. Christou, *J. Appl. Phys.* **2002**, *91*, 7158 – 7160.
[7] K. Takeda, K. Awaga, T. Inabe, A. Yamaguchi, H. Ishimoto, T. Tomita, H. Mitamura, T. Goto, N. Mori, H. Nojiri, *Phys. Rev. B* **2002**, *65*, 094424.
[8] Y. Murata, K. Takeda, T. Sekine, M. Ogata, K. Awaga, *J. Phys. Soc. Jpn.* **1998**, *67*, 3014 – 3017.
[9] Y. Suzuki, K. Takeda, K. Awaga, *Phys. Rev. B* **2003**, *67*, 132402.

[10] M. Evangelisti, J. Bartolomé, *J. Magn. Magn. Mater.* **2000**, *221*, 99 – 102.
[11] A. Sieber, G. Chaboussant, R. Bircher, C. Boskovic, H.-U. Güdel, G. Christou, H. Mutka, *Phys. Rev. B* **2004**, *70*, 172413.
[12] D. Gatteschi, L. Sorace, *J. Solid State Chem.* **2001**, *159*, 253 – 261.
[13] B. Barbara, L. Thomas, F. Lionti, I. Chiorescu, A. Sulpice, *J. Magn. Magn. Mater.* **1999**, *200*, 167 – 181.
[14] T. Lis, *Acta Crystallogr. Sect. B* **1980**, *36*, 2042 – 2046.

